Journal of Alloys and Compounds 508 (2010) 520–522

Contents lists available at ScienceDirect

Journal of Alloys and Compounds

journal homepage: www.elsevier.com/locate/jallcom

Enhanced ferroelectric properties in $BiFe_{0.95}Mn_{0.05}O_3$ thin films

Shougang Cui *

Jinan Yuantek Sol-Gel Technology Ltd., Shandong 250010, People's Republic of China

ARTICLE INFO

Article history:
Received 4 April 2010
Received in revised form 20 August 2010
Accepted 26 August 2010
Available online 22 September 2010

Keywords:
Mn-doped $BiFeO_3$
Ferroelectrics
Thin films
Aging
Defect complexes

ABSTRACT

The $BiFe_{0.95}Mn_{0.05}O_3$ (BFMO) thin films were deposited on Pt/Ti/SiO_2/Si substrates using a metal organic decomposition process combined with a sequential layer annealing method. The BFMO film annealed for 10 min/layer exhibits a much larger remanent polarization ($P_r \sim 81\ \mu C/cm^2$), a lower coercive field ($E_c \sim 178$ kV/cm), as well as stronger charge-retaining ability and fatigue resistance in comparison with that annealed for 2 min/layer, demonstrating that prolonging the annealing time can favor the improvement of the ferroelectric properties of BFMO film. These results are discussed based on the phase transition as well as the formation of defect complexes between oxygen vacancies and acceptors during the annealing treatment.

1. Introduction

$BiFeO_3$ (BFO) is one of the most intensively studied multiferroic materials [1–8], and has been demonstrated to be a promising lead-free candidate for ferro- and piezoelectric devices. However, the severe leakage problem and large coercive field (E_c) of BFO-based films may hinder its future application in devices. A lot of efforts have been made to decrease the leakage current of BFO-based film prepared by the chemical solution deposition method [9–12]. Among these efforts, the isovalent-ion substitution of Mn^{3+} at Fe^{3+} sites has been verified to be an effective method not only for reducing leakage current but also for enhancing the ferroelectric properties of BFO films. Unfortunately, the reported Mn-doped BFO films exhibit a large coercive field ($E_c > 300$ kV/cm) [13,14]. Considering that the BFO-based films may be aged to some extent due to the formation of defect complexes between oxygen vacancies [$(V_{O^{2-}})^{\bullet\bullet}$] and acceptors [$(A^{2+}_{Fe^{3+}})'$], such as $(Fe^{2+}_{Fe^{3+}})'$ or $(Mn^{2+}_{Fe^{3+}})'$ [15,16], it is natural to consider that such a large E_c is not an intrinsic characteristic of BFO but should be due to that the ferroelectric domains in the aged films are stabilized by the local field produced by defect complexes. Thus, E_c could be reduced to a great extent through decreasing the content of $(V_{O^{2-}})^{\bullet\bullet}$ in the film. It is well known that prolonging the annealing time can favor grain growth of the film, which should in turn reduce the grain boundaries as well as the content of $(V_{O^{2-}})^{\bullet\bullet}$, since that the $(V_{O^{2-}})^{\bullet\bullet}$ are prone to locating at the grain boundaries. That is, prolonging the annealing time should have a positive effect on deaging the film. On the other hand, prolonging the annealing time could accelerate the diffusion of $(V_{O^{2-}})^{\bullet\bullet}$ in the film, which may in turn lead to the full aging of the film. Therefore, the above mentioned positive and negative effects resulting from prolonging the annealing time on the aging of BFO-based films should be investigated to clarify which effect is dominant.

In the present work, the ferroelectric properties of the $BiFe_{0.95}Mn_{0.05}O_3$ (BFMO) film annealed for 2 min/layer ($BFMO_{2\,min}$) and BFMO film annealed for 10 min/layer ($BFMO_{10\,min}$) were comparatively investigated. The enhanced ferroelectric properties for the $BFMO_{10\,min}$ film demonstrate that prolonging the annealing time can favor the deaging of the BFMO film.

2. Experimental procedure

The BFMO thin films were deposited on Pt/Ti/SiO_2/Si substrates using a metal organic decomposition process. The precursor solution was prepared by dissolving bismuth nitrate, iron nitrate and manganese acetate in acetic acid and ethylene glycol. Each layer of the $BFMO_{10\,min}$ film was deposited onto the substrate by spin coating at 6000 rpm for 20 s. Each layer was pyrolyzed at 400 °C for 10 min in air and annealed at 525 °C for 10 min in N_2 atmosphere. These steps were repeated several times before the desired thickness (600 nm) was obtained. For comparison, $BFMO_{2\,min}$ film with each layer annealed at 525 °C for 2 min in N_2 was also fabricated. Au top electrodes were deposited on the films using a sputtering system through a shadow mask with a diameter of 200 μm for electrical measurements. The crystal structures of the BFMO films were characterized by an X-ray diffractometer (XRD, D8, Bruker, Germany). The surface morphologies of the films were detected using an atomic force microscope (AFM, NSIV, Veeco, NY) in the tapping mode. A standard ferroelectric tester (Radiant Technologies, Albuquerque, NM) was used to measure the ferroelectric properties at room temperature.

* Corresponding author. Tel.: +86 53187155535; fax: +86 53187155535.
E-mail address: cuishougang@gmail.com.

0925-8388/$ – see front matter © 2010 Elsevier B.V. All rights reserved.
doi:10.1016/j.jallcom.2010.08.108

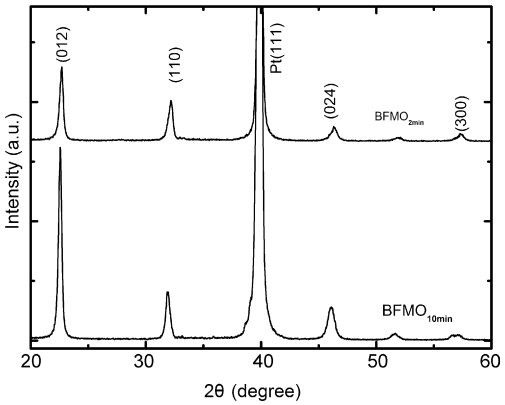

Fig. 1. XRD patterns of $BFMO_{10\,min}$ and $BFMO_{2\,min}$ films.

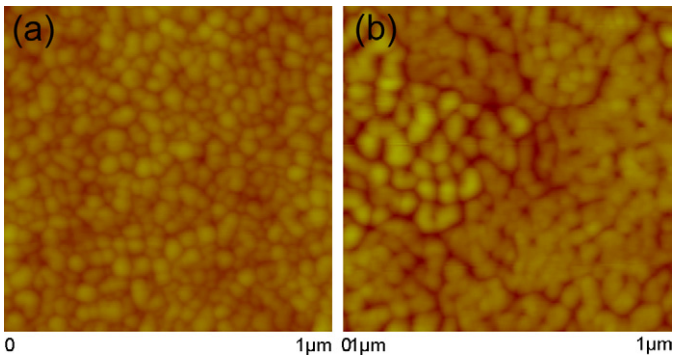

Fig. 2. AFM images of (a) $BFMO_{2\,min}$ film and (b) $BFMO_{10\,min}$ film.

3. Results and discussions

Fig. 1 shows XRD patterns of the $BFMO_{10\,min}$ film and the $BFMO_{2\,min}$ film. It can be found that both films exhibit similar polycrystalline structures except the differences in the relative intensity and the full width at half-maximum (FWHM) of (0 1 2) peak. The relative intensity of (0 1 2) peak for the $BFMO_{10\,min}$ film is much stronger than that of $BFMO_{2\,min}$ film, while the FWHM of the (0 1 2) peak for the former (0.305) is smaller than that of the latter (0.349). This should be due to that the grain growth induced by the minimization of surface and grain boundary energies occurs through the motion of grain boundaries during the course of prolonging the annealing time [Note that the (0 1 2) plane has the lowest surface energy among all facets of the lattice.] [17].

An evident difference of the grain size can be observed from the surface morphologies in the AFM images shown in Fig. 2. The root mean square (rms) roughnesses for $BFMO_{2\,min}$ and $BFMO_{10\,min}$ films are 2.375 and 3.424 nm, respectively. The larger rms roughness of the latter should be due to its larger grain size compared with the former, which is consistent with the XRD results.

Fig. 3(a) and (b) show the electric field dependence of *P–E* hysteresis loops for $BFMO_{10\,min}$ and $BFMO_{2\,min}$ films. It can be found that the *P–E* hysteresis loops for $BFMO_{10\,min}$ film show higher rectangularity (P_r/P_s equals to 92%) than that (83%) of $BFMO_{2\,min}$ film at electric field of 500 kV/cm. Note that the P_r value (~81 μC/cm^2) of $BFMO_{10\,min}$ film is about 53% larger than that (~53 μC/cm^2) of $BFMO_{2\,min}$ film, while the E_c value (~178 kV/cm) of the former is about 10% smaller than that (~204 kV/cm) of the latter. It is well known that the P_s vector is along $(1\,1\,1)_c$ direction for the BFO with a rhombohedral structure. The P_r ratio between the (1 1 0) orientation and the (0 1 2) $[(0\,0\,1)_c]$ orientation was $\sqrt{2}/1$ [1,18]. Accordingly, the stronger relative intensities of (0 1 2) peak in $BFMO_{10\,min}$ film indicate that its P_r value should be lower than that of $BFMO_{2\,min}$ film. It is contrary to the results shown in Fig. 3(a) and (b). This indicates that a phase transition from the distorted rhombohedral to tetragonal structure should occur in BFMO films [19,20], leading to that the P_s vector may be converted from $(1\,1\,1)_c$ direction into (0 1 2) [i.e., $(0\,0\,1)_t$ indexed using the tetragonal symmetry] direction. Nevertheless, the difference of the relative

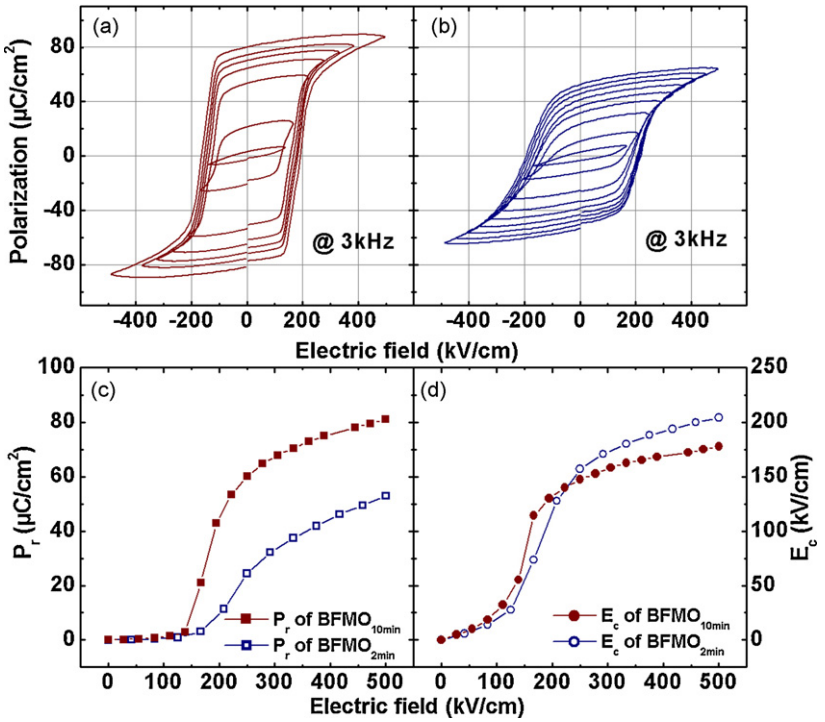

Fig. 3. Room temperature ferroelectric properties of $BFMO_{10\,min}$ and $BFMO_{2\,min}$ films. *P–E* hysteresis loops as a function of the electric field of (a) $BFMO_{10\,min}$ film; (b) $BFMO_{2\,min}$ film; (c) P_r and (d) E_c as a function of the electric field for both films.

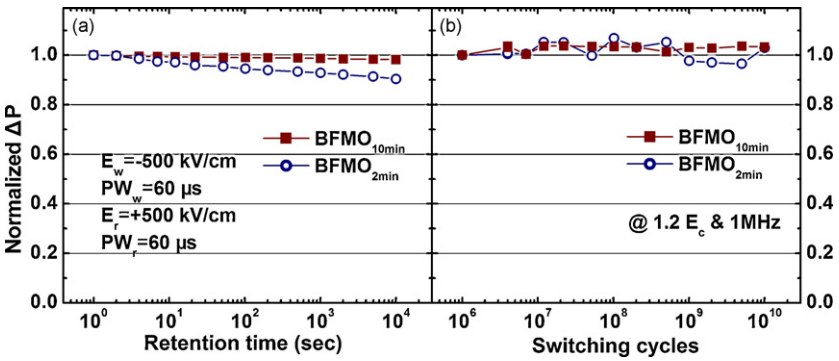

Fig. 4. Room temperature ferroelectric properties of $BFMO_{10\,min}$ and $BFMO_{2\,min}$ films: (a)The pulsed polarization (normalized ΔP) as a function of retention time for both films and (b)The normalized ΔP as a function of switching cycles for both films.

intensity of (0 1 2) peaks in these two films can hardly account for such a large distinction of the P_r value. There should be other crucial factors affecting the ferroelectric properties. Note that the BFMO films in this work were annealed in N_2 at 525 °C that was much lower than the Curie temperature of BFO (850 °C). Therefore, aging can inevitably occur because of the formation of defect complexes between $(V_{O^{2-}})^{\bullet\bullet}$ and $(A^{2+}_{Fe^{3+}})'$ [15,16]. The polarization (P_D) of defect complexes can align along the direction of P_S during aging [21], which in turn provides a driving force to hinder the switching of ferroelectric domains and eventually reverse as-switched domains to their original orientations (i.e., domain backswitching) [16]. Therefore, the larger P_r value of $BFMO_{10\,min}$ film than that of $BFMO_{2\,min}$ film should be due to the less defect complexes formed during the annealing treatment, which should result from the less $(V_{O^{2-}})^{\bullet\bullet}$ because of the smaller volume fraction of grain boundaries. This demonstrates that prolonging the annealing time is an effective method for deaging the film. On the other hand, the negative effect resulting from the diffusion of $(V_{O^{2-}})^{\bullet\bullet}$ as mentioned in introduction can be ruled out in $BFMO_{10\,min}$ film, since that the diffusion of $(V_{O^{2-}})^{\bullet\bullet}$ can be accomplished in a short time.

The dependence of P_r and E_c value on the electric field are also plotted for clarity as illustrated in Fig. 3(c) and (d), respectively. The P_r and E_c for $BFMO_{10\,min}$ film are readily to become saturated compared with those for $BFMO_{2\,min}$ film. This can be attributed to be the lower E_c for $BFMO_{10\,min}$ film resulting from the adequate and uniform grain growth. The broad distribution of E_c value for $BFMO_{2\,min}$ film should be due to that the increased leakage current originated from the gradual release of $(V_{O^{2-}})^{\bullet\bullet}$ from the defect complexes lead to the decrease of effective electric field applied on the film.

As shown in Fig. 4(a), the loss of the pulsed polarization [$\Delta P = P^*$ (switched polarization) $- P\hat{}$ (nonswitched polarization)] for $BFMO_{10\,min}$ film for the retention time up to 10^4 s is only 2%, which is about one-fifth of that for $BFMO_{2\,min}$ film. This provides an evidence for the much weaker driving force resulting from the less defect complexes in the former than that of the latter. On the other hand, both films exhibit almost the same fatigue-free behavior although $BFMO_{2\,min}$ film exhibits an 8% polarization loss in retention test [see Fig. 4(b)]. It has been proposed by Hu et al. that the defects complexes of $(A^{2+}_{Fe^{3+}})' - (V_{O^{2-}})^{\bullet\bullet}$ can be broken by the applied electric field [11]. However, the movement of the released $(V_{O^{2-}})^{\bullet\bullet}$ during the fatigue test will be greatly limited by $(A^{2+}_{Fe^{3+}})'$ through the recombination with $(V_{O^{2-}})^{\bullet\bullet}$, meaning that few oxygen vacancies can reach the interface between the electrode and BFMO films during the electric field cycling. It is worth noting that, in contrast to the obvious fatigue behaviors in Zn-doped BFO film reported by Hu et al. [11], the strong fatigue resistance in $BFMO_{2\,min}$ film can be ascribed to the less $(V_{O^{2-}})^{\bullet\bullet}$ released from the defect complexes, because the electric field (1.2 E_c) adopted for fatigue test in the present work is much lower than those utilized by Hu et al. (note that the E_c for $BFMO_{2\,min}$ film is about 33% lower than that of Zn-doped BFO film).

4. Conclusions

In summary, the ferroelectric properties of $BFMO_{2\,min}$ and $BFMO_{10\,min}$ films were comparatively investigated. Phase transition from the distorted rhombohedral to tetragonal structure should occur in BFMO films, leading to that the P_s vector may be converted from $(1\,1\,1)_c$ direction into $(0\,1\,2)$ [i.e., $(0\,0\,1)_t$ indexed using the tetragonal symmetry] direction. The $BFMO_{10\,min}$ film exhibits a larger P_r value (~81 μC/cm^2) and smaller E_c value (~178 kV/cm) in comparison with $BFMO_{2\,min}$ film. This should be due to the higher relative intensity of (0 1 2) peak and less defect complexes formed in the former compared with those of the latter. This demonstrates that prolonging the annealing time is an effective method for deaging the BFMO film.

References

[1] J. Wang, J.B. Neaton, H. Zheng, V. Nagarajan, S.B. Ogale, B. Liu, et al., Science 299 (2003) 1719–1722.
[2] T. Zhao, A. Scholl, F. Zavaliche, K. Lee, M. Barry, A. Doran, et al., Nat. Mater. 5 (2006) 823–829.
[3] J. Dho, X. Qi, H. Kim, J.L. MacManus-Driscoll, M.G. Blamire, Adv. Matter 18 (2006) 1445–1448.
[4] J. Seidel, L.W. Martin, Q. He, Q. Zhan, Y.H. Chu, A. Rother, et al., Nat. Mater. 8 (2009) 229–234.
[5] R.J. Zeches, M.D. Rossell, J.X. Zhang, A.J. Hatt, Q. He, C.-H. Yang, Science 326 (2009) 977–980.
[6] C.H. Yang, J. Seidel, S.Y. Kim, P.B. Rossen, P. Yu, M. Gajek, et al., Nat. Mater. 8 (2009) 485–493.
[7] T. Choi, S. Lee, Y.J. Choi, V. Kiryukhin, S.W. Cheong, Science 324 (2009) 63–66.
[8] X.M. Chen, G.D. Hu, W.B. Wu, C.H. Yang, X. Wang, J. Am. Ceram. Soc. 93 (2010) 948–950.
[9] S.K. Singh, K. Maruyama, H. Ishiwara, Appl. Phys. Lett. 91 (2007) 112913–112923.
[10] G.D. Hu, X. Cheng, W.B. Wu, C.H. Yang, Appl. Phys. Lett. 91 (2007) 232909–232913.
[11] G.D. Hu, S.H. Fan, C.H. Yang, W.B. Wu, Appl. Phys. Lett. 92 (2008) 192905–192913.
[12] X.M. Chen, G.D. Hu, J. Yan, X. Wang, C.H. Yang, W.B. Wu, J. Phys. D: Appl. Phys. 41 (2008) 225402(5).
[13] S.K. Singh, H. Ishiwara, K. Maruyama, Appl. Phys. Lett. 88 (2006) 262908–262913.
[14] Z. Wen, G.D. Hu, S.H. Fan, C.H. Yang, W.B. Wu, Y. Zhou, et al., Thin Solid Films 517 (2009) 4497–4501.
[15] S.G. Cui, G.D. Hu, W.B. Wu, C.H. Yang, L.L. Jiao, Z. Wen, J. Am. Ceram. Soc. 92 (2009) 1610–1612.
[16] Z. Wen, G. Hu, C. Yang, W. Wu, Appl. Phys. A 97 (2009) 937–941.
[17] J. Yan, G.D. Hu, X.M. Chen, W.B. Wu, C.H. Yang, J. Appl. Phys. 104 (2008) 076103–76113.
[18] J. Li, J. Wang, M. Wuttig, R. Ramesh, N. Wang, B. Ruette, et al., Appl. Phys. Lett. 84 (2004) 5261–5263.
[19] S.K. Singh, H. Ishiwara, K. Sato, K. Maruyama, J. Appl. Phys. 102 (2007) 094109–94113.
[20] C. Ederer, N.A. Spaldin, Phys. Rev. Lett. 95 (2005) 257601(4).
[21] L.X. Zhang, X.B. Ren, Phys. Rev. B 73 (2006) 094121–94126.